J Mater Sci (2012) 47:2078–2087
DOI 10.1007/s10853-011-6006-6

Polyester textile functionalization through incorporation of pH/thermo-responsive microgels. Part II: polyester functionalization and characterization

Pelagia Glampedaki · Alfredo Calvimontes · Victoria Dutschk · Marijn M. C. G. Warmoeskerken

Received: 12 July 2011 / Accepted: 27 September 2011 / Published online: 12 October 2011

Abstract A new approach to functionalize the surface of polyester textiles is described in this study. Functionalization was achieved by incorporating pH/temperature-responsive polyelectrolyte microgels into the textile surface layer using UV irradiation. The aim of functionalization was to regulate polyester wettability according to ambient conditions by imparting stimuli-responsiveness from the microgel to the textile itself. Microgels consisted of pH/thermo-responsive microparticles of poly(*N*-isopropylacrylamide-*co*-acrylic acid) either alone or complexed with the pH-responsive natural polysaccharide chitosan. Scanning Electron Microscopy, X-ray Photoelectron Spectroscopy, ζ-potential measurements, and topographical analysis were used for surface characterization. Wettability of polyester textiles was assessed by dynamic wetting, water vapor transfer, and moisture regain measurements. One of the main findings showed that the polyester surface was rendered pH-responsive, both in acidic and alkaline pH region, owing to the microgel incorporation. With a marked relaxation in their structure and an increase in their microporosity, the functionalized textiles exhibited higher water vapor transfer rates both at 20 and 40 °C, and 65% relative humidity compared with the reference polyester. Also, at 40 °C, i.e., above the microgel Lower Critical Solution Temperature, the functionalized polyester textiles had lower moisture regains than the reference. Finally, the type of the incorporated microgel affected significantly the polyester total absorption times, with an up to 300% increase in one case and an up to 80% decrease in another case. These findings are promising for the development of functional textile materials with possible applications in biotechnology, technical, and protective clothing.

P. Glampedaki (✉) · V. Dutschk · M. M. C. G. Warmoeskerken
Engineering of Fibrous Smart Materials (EFSM), Faculty of Engineering Technology (CTW), University of Twente, P.O. Box 217, 7500 AE Enschede, The Netherlands
e-mail: p.glampedaki@utwente.nl

A. Calvimontes
Polymer Interfaces, Leibniz-Institut für Polymerforschung Dresden e.V., Hohe Str. 6, 01069 Dresden, Germany

Introduction

Functionalization of textiles has been the aim of many studies in the field of intelligent materials. Biomimesis (lotus, pinecone effect, etc.), integrating informatics into textile production (incorporation of computer-controlled electronic sensors), creating new fibers either natural or synthetic (algae biocomposite, ferroelectric polymeric, etc.), and convergence of opposites (e.g., hydrophilic with hydrophobic materials) are some of the approaches used for textile functionalization [1–4]. Though such technologies help create new advanced materials, there is often the drawback that multiple reaction steps or large consumption of reagents are needed for in situ preparation. Consequently, purification of the final products can become a laborious and time-consuming process. Other times, a customized set-up may be required increasing production costs. Furthermore, the final effect may be short termed (e.g., when plasma treatment is used for creating radicals [5]) or permanent (e.g., hydrophobization coatings of cotton [6]) with no option for dynamic changes in properties.

This study focuses on a novel approach toward textile surface functionalization: the use of hydrophilic surface modifying systems based on polyelectrolyte microgels for rather hydrophobic polyester textiles. The proposed technique involves simple steps and equipment, and the microgels are prepared outside the functionalization

procedure offering versatility in composition and easiness in the final cleaning step. Furthermore, using stimuli-responsive microgels for polyester functionalization offers a unique advantage: the on-demand enhancement of the textile moisture/water management properties. Microgels are, in fact, hydrogels in the form of microparticulate suspensions and they contain by definition large amounts of water. Therefore, microgel-functionalized polyesters are expected to exhibit increased wettability under certain conditions. Moreover, pH/thermo-responsive microgels attract or expel water according to the ambient conditions of pH and temperature [7–9]. Hence, polyester textiles functionalized with stimuli-responsive microgels are expected to exhibit not only improved but also, more importantly, controlled moisture/water management properties, depending on the demands of their surrounding environment. Such a functionalization technology offers new opportunities for the development of functional synthetic textiles, applicable to biomedical and protective clothing.

In this study, the microgels used consist of pH/thermo-responsive microparticles of poly(*N*-isopropylacrylamide-*co*-acrylic acid) (PNIAA) either alone in suspension (microgel **M**) or in the form of polyelectrolyte complexes with chitosan (microgel **CM**). Chitosan is a natural pH-responsive polysaccharide with multiple applications in biomedicine [10] and its complexation with PNIAA was engineered so that the pH/thermo-responsiveness of the resulting microgel **CM** would be exhibited within a physiological pH and temperature range. The microgel preparation, morphology, and physicochemical characterization are reported in detail elsewhere [11]. The aim was to functionalize polyester textiles with these microgels so that their imparted pH/thermo-responsiveness would be exhibited ultimately at temperatures close to the average human body temperature and at pH values close to the average pH of human skin.

Incorporation of the microgels into polyester surface layers was conducted using UV irradiation in the presence of the photoinitiator benzophenone. Benzophenone is known to produce macroradicals by hydrogen-abstraction reactions, when irradiated at low wavelengths [12]. In this study, the concept was to photocrosslink, therefore anchor, the microgels on polyester in order to covalently—thus, durably—bind the functionalizing system with the textile. Photocrosslinking of polymers (i.e., irradiation subsequent to polymerization) is used in many variations to create inter-polymer networks (e.g., to produce hydrogels directly from polymer solutions [13]) and control the morphology and properties of polymer blends, membranes, etc. [14, 15]. The main requirement is the use of polymers with hydrogen-donor moieties. Poly(ethylene terephthalate) (PET) is the polyester type chosen for this study, as it is highly photoreactive [16, 17]; poly(acrylic acid), which is a main component of PNIAA, has abstractable hydrogen atoms attached to the tertiary carbon atoms of its chains [12]; amide groups, in which PNIAA is rich owing to its *N*-isopropylacrylamide units, are generally susceptible to photocleavage under certain conditions [18, 19]; finally, chitosan has wavelength-dependent photosensitivity and at 260 nm it undergoes possibly deacetylation, as well as chain scission at the glucosidic linkage [20]. With the above in mind, it is evident that there are multiple possibilities of photocrosslinking in the systems under study, and microgel presence on polyester is not expected to be a result of mere physical adsorption.

Experimental

Materials

Woven polyester textiles from poly(ethylene terephthalate) (PET, Verosol) had flat yarns in the warp direction and textured in the weft direction, with a fineness of 72 and 167 dTex, respectively. The textile density was 38.5 ± 1.5 threads per cm in the warp direction and 22 ± 1.5 threads per cm in the weft direction. The textile weight per unit area was 73 ± 3 g/m^2. Benzophenone (Acros Organics) was used as a photoinitiator for the microgel incorporation in the polyester surface layer. A non-ionic detergent (Tanaterge EP5071, Tanatex) was used for washing. All other reagents were of analytical grade.

Microgel incorporation into polyester surface layer

Polyester textile pieces of dimensions 4 cm × 12 cm were first impregnated with benzophenone solution (0.05 M in 90% ethanol). Then, the samples were air dried and subsequently immersed into 20 mL of microgel for 1 h. After impregnation, the textile samples were placed on a clean Teflon substrate and were irradiated using a ultra-violet (UV) lamp (Distrilab B.V., The Netherlands) at 254 nm for 30 min. Then, the samples were washed with a detergent solution of 5 g/L Tanaterge EP 5071 and 2 g/L Na_2CO_3 at 50:1 liquor-to-goods ratio. Washing was performed with a Linitest (SDL Atlas, United Kingdom) apparatus under mild rotation at 60 °C for 30 min. Finally, the samples were air dried and kept in a desiccator until further use. The dry add-ons of microgels **M** and **CM** on polyester textiles were determined to be approximately 0.4 and 0.6 wt%, respectively. The sample codes and description are given in Table 1.

Polyester surface analysis and physicochemical characterization

A High Resolution Scanning Electron Microscope LEO 1550 (Carl ZEISS, Germany) was used to observe the

Table 1 Polyester textile samples under study

Sample code	Description
PET R	Reference (R)
PET RM	Functionalized with PNIAA microgel (**M**)
PET RCM	Functionalized with PNIAA/chitosan microgel (**CM**)

polyester surface morphology. Samples were glued with double-face tape on the sample holder and were gold sputtered prior to analysis.

The polyester surface chemical composition was determined by X-ray Photoelectron Spectroscopy (XPS) using a Quantera Scanning Microprobe spectrometer (Physical Electronics, USA). The samples were irradiated with monochromatic Al Kα X-rays (1486.6 eV) at 25 W. The standard beam and detector input angle was 45°. Survey spectra were recorded from −5 to 1345 eV with pass energy of 224 eV and a step of 0.8 eV. Spectra fitting was done with respect to the reference binding energy of the aliphatic carbon 1*s* orbital at 284.8 eV.

The ζ potential of polyester textiles was determined with streaming potential measurements performed using an Electro Kinetic Analyzer (EKA, Anton Paar). The procedure is described in Ref. [21]. The measuring cell was cylindric with a 26 mm diameter. The electrode solution was 10^{-3} mol/L KCl and titration was performed in the pH range 3–10 using 0.1 M HCl and 0.1 M KOH.

The surface topography of the polyester samples was analyzed using an optical non-contact 3D-scanner, MicroGlider (FRT, Germany), operating on the principle of the chromatic aberration of light. The measuring principle and related calculations are described in detail in references [22, 23]. Waviness and porosity were determined based on images of dimensions 2 mm × 2 mm. Filament microroughness was determined for a measuring length of 50 μm.

Dynamic wetting measurements based on the sessile drop method were carried out with a FibroDAT 1122HS dynamic contact angle tester (Fibro System, Sweden), equipped with a high speed video camera, in an environment of controlled temperature and humidity of 23 ± 1 °C and 50 ± 4%, respectively. 13 μL drops of water or buffer solution (pH 4 or 8) were applied to the textile surface by a short stroke from an electromagnet. After deposition of the drop, data were collected for 150 s. The time needed for the drop to disappear from the sample surface, as determined by the imaging system, equals to the total absorption time for each textile sample. The values obtained were the average of five measurements.

Water vapor transmission (WVT) measurements were performed according to the standard UNI 4818-26 using aluminum containers filled with 25 mL water each. The container lids had a round opening of 1000 mm^2 to allow vapor exhaust during testing. Polyester samples of 40 mm diameter were placed under the lid openings and the containers were then weighed. A bench top test chamber SM-1.0-3800 (Thermotron, USA) was used for conditioning the samples for 24 h at 20 and 40 °C, and at 65 and 95% relative humidity (RH). After each conditioning run, the containers were weighed again and the difference in weight before and after 24 h was used to calculate the water vapor transmission rate (WVTR), according to Eq. 1:

$$\text{WVT rate} = \frac{\Delta m \times 24}{S \times t} \quad (1)$$

where Δm is the change of weight in grams, S is the testing surface area in m^2 (which has a constant value of 1000 mm^2), and t is the test time in hours. The values obtained were the average of three measurements.

Moisture regain (M_R, %) was determined by weight measurements. The samples were first dried at 105 °C for 1 h and weighed (W_d) with a high precision WXS analytical balance (Mettler-Toledo, The Netherlands). Conditioning the samples followed for 24 h at certain temperature (20 or 40 °C) and RH (65, 75, 85, or 95%) in the above-mentioned test chamber and the samples were weighed again (W_{T-RH}). The M_R was calculated using Eq. 2:

$$M_R = \frac{W_{T-RH} - W_d}{W_d} \times 100 \quad (2)$$

Results and discussion

Polyester textile functionalization and surface characterization

As reported in Ref. [11], microgels **M** and **CM** are responsive toward changes within the physiological pH and temperature range. Their Lower Critical Solution Temperatures (LCSTs) are approximately 34 and 36 °C, and their isoelectric points appear at pH 3.4 and 6, respectively [11]. In order to investigate the incorporation of microgels **M** and **CM** into the surface layer of polyester textiles, SEM and XPS were employed. The surface morphology of the polyester textile samples was examined first, in order to confirm the presence of microparticles or complexes on the fibers.

Compared with reference polyester PET R (Fig. 1a), functionalized polyester samples PET RM (Fig. 1b) and PET RCM (Fig. 1c) have spheroid and circular formations, respectively, uniformly distributed on their fibers. In SEM image 1a, the angular pieces that protrude from the reference polyester fiber surface are oligomers resulting from the fiber production process and they unavoidably leach out from the fiber bulk, even after the samples have been thoroughly washed. Figure 1b depicts the incorporation of PNIAA microparticles into the polyester fiber surface in a

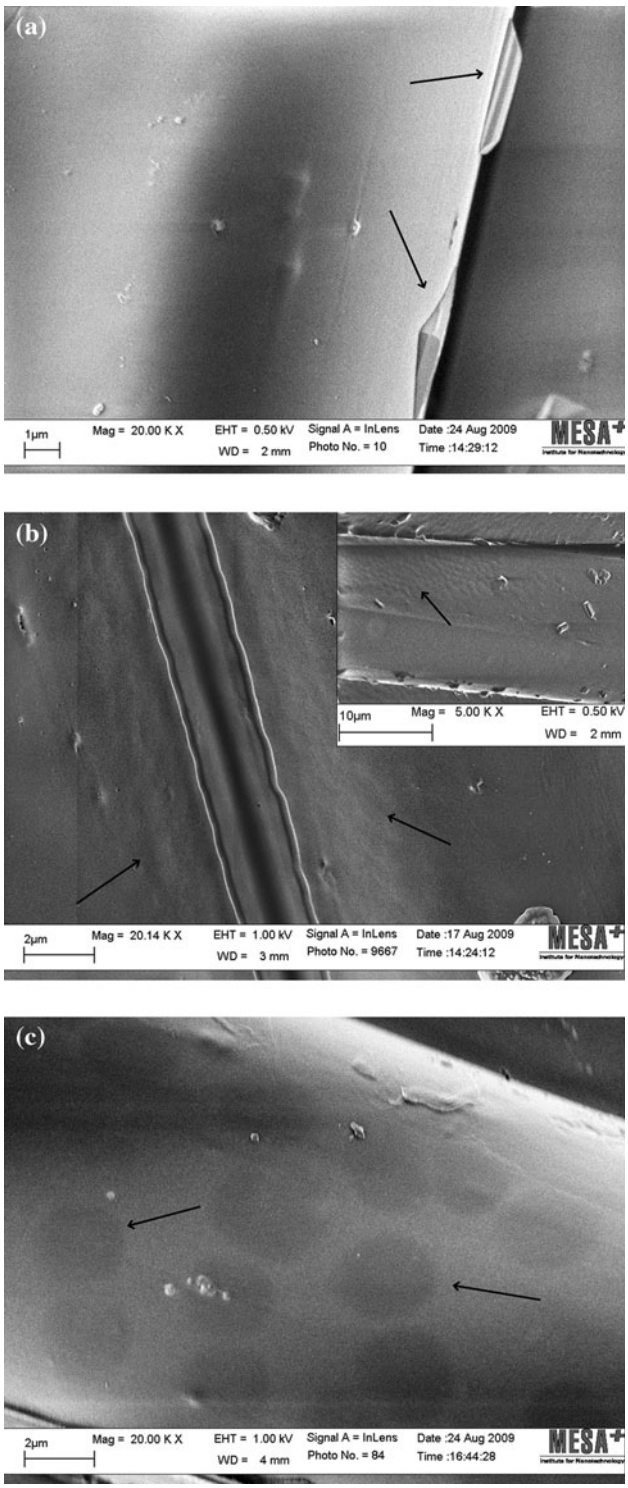

Fig. 1 High resolution SEM images of polyester: **a** reference (PET R); **b** functionalized with microgel **M** (PET RM); **c** functionalized with microgel **CM** (PET RCM)

closely packed and apparently continuous layer. The inset in Fig. 1b is an image of PET RM at lower magnification, which depicts more clearly the PNIAA microparticles on polyester fibers. Arrows are used to point areas of interest. The result is much different in the case of **CM** incorporation (Fig. 1c), where the PNIAA/chitosan complexes appear as darker, non-voluminous imprints of circular shape, completely integrated, and more sparsely distributed on the fiber surface compared with **M** incorporation of Fig. 1b. In the latter case, PNIAA microparticles are estimated to have a diameter of less than 1 μm (∼900 nm) which approximates the estimated diameter of air-dried microparticles on a silicon wafer [11]. The reason that on the polyester fiber the microparticles appear smaller is that they are densely accumulated one next to another and so there is not enough space for them to completely collapse and flatten. On the contrary, this effect appears in the case of the **CM** complexes which have an estimated diameter of about 2 μm. **CM** complexes are more sparsely distributed on the fibers than **M** particles and, therefore, have more space to stretch out completely their collapsed structure.

Based on dynamic surface tension measurements (data from measurements at the water/air interface were not shown in this study), both PNIAA microparticles and **CM** complexes were found to be surface active. Hence, they are both expected to have affinity for polyester and be evenly distributed on its fibers. However, during preparation of microgel **CM**, complexation of PNIAA with chitosan leads to contraction of the PNIAA microparticles due to electrostatic attraction. At the same time, dilution of microgel **M** takes place, as 1 volume of microgel **M** is mixed with 2.5 volumes of chitosan solution. Therefore, in a certain volume of microgel **CM** there are fewer PNIAA microparticles present than in the same volume of microgel **M**. Hence, when polyester is impregnated with the two microgels using the same liquor-to-cloth ratio in both cases, fewer microparticles—thus, **CM** complexes—are expected to be found on its fibers when microgel **CM** is used. This effect is depicted in Fig. 1c, in contrast with Fig. 1b.

To analyze the chemical composition of the functionalized polyester textiles, XPS was used and the results are shown in Tables 2 and 3. The first significant and obvious, based on the data, finding is the presence of nitrogen on the surface of PET RM and PET RCM, attributed to the amide groups of PNIAA and the amine groups of chitosan. Also, a significant decrease in the total atomic concentration of oxygen is revealed, compared with PET R (Table 2). Owing to the simultaneous increase in total carbon atoms attributed to the polymeric backbones of PNIAA and chitosan, the N/C and O/C atomic ratios between PET RM and PET RCM do not differ significantly (Table 2).

From the XPS deconvolution data of Table 3, it is derived that reference polyester has three types of bound oxygen atoms; O1, corresponding to double-bonded

Table 2 Elemental composition of the polyester surfaces determined by XPS

Polyester samples	Total atomic concentration (%)			Atomic ratios	
	C 1*s*	N 1*s*	O 1*s*	N/C	O/C
PET R	73.2	–	26.8	–	0.37
PET RM	74.8	6.8	18.4	0.09	0.26
PET RCM	74.0	4.1	21.9	0.06	0.30

oxygen (carbonyl group); O2, to single-bonded oxygen of an ester group; and O3, to single-bonded oxygen of an alcohol end group. The corresponding bands of the deconvolution spectrum for oxygen (not shown) were attributed to binding energies shifted with respect to the aliphatic carbon binding energy (284.8 eV). O1 and O2 have practically the same atomic concentration (at.%), as they both belong to the ester (**O**=C–**O**) or carboxyl (**O**=C–**O**H) groups of PET with a ratio 1:1. The third type of oxygen atom belongs to the alcohol end groups of PET (C–**O**H) and the fact that it is absent from the surface of PET RM and PET RCM indicates that all the hydroxyl end groups have reacted probably with carboxyl groups of PNIAA forming ester bonds. The O3 absence could also be caused by partial polyester photodegradation [16, 24] but a more in-depth analysis is needed to confirm or reject this possibility, taking into consideration all conditions of UV irradiation (wavelength, duration, presence of microgel, etc.). In any case, the increased O1 at.% determined for PET RM (64.0% compared with 46.7% of PET R) and PET RCM (64.3% compared with 46.7% of PET R) corroborates the presence of PNIAA on the fiber surface because it can be attributed to the multiple carbonyl groups of the PNIAA amide bonds. The carboxyl groups of acrylic acid in the PNIAA structure contribute also to the above-mentioned increase; however, their amount is not comparable with that of the amide groups in the PNIAA backbone and for that reason the O2 at.% does not show the same increase as O1 at.%.

With respect to the differently bound carbon atoms, the deconvolution spectra (not shown) depicted five bands designated to equal carbon atom types (C1–C5, Table 3). The corresponding binding energies for each atom on each polyester sample are given in Table 3. As expected, C2 (with a binding energy of 284.8 eV) has the highest atomic concentration for all polyester samples, and corresponds mainly to the carbon atoms of the PET aromatic ring (**C–C**, **C–**H). C3 corresponds to aliphatic carbon atoms single-bonded with oxygen (–**C**H_2–O), and C5 to carbonyl carbon atoms, i.e., double-bonded with oxygen (**C=**O), attributed to ester, carboxyl or amide groups depending on the sample. These data correspond well with relevant bibliography [25–27]. There are two more types of carbon atoms, designated as C1 and C4, derived from the deconvolution spectra of all polyester samples which are not usually encountered in PET XPS spectra. C4 with a binding energy of ca. 287 eV has been reported also elsewhere [25] where it is attributed to another type of oxidized carbon atom with no further specification. C1, on the other hand, with no obvious origin is possibly a product of impurities or an artifact of the measurement. Even though trends can be drawn among samples PET R, PET RM, and PET RCM for the carbon and oxygen atomic concentrations (e.g., the atomic concentrations of C2, C3, and O1 increase but those of C5 and O2 decrease), it is very difficult to distinguish among the contributions of each component (chitosan, PNIAA, PET) based on the above data alone.

However, assumptions can be made regarding the surface coverage of polyesters by microgels **M** and **CM** based on theoretical values presented in Table 4. Since nitrogen is present in both microgels but not on PET, its ratio to carbon (N/C) can be used to estimate to what extent the polyester surfaces are covered by microgels. To this end, the theoretical values of atomic concentrations and ratios in Table 4 were calculated based on the assumption that the repeating units of *N*-isopropylacrylamide and acrylic acid

Table 3 XPS deconvolution data for the differently bound carbon and oxygen atoms of the surface of polyester samples PET R, PET RM, and PET RCM

Polyester samples	XPS parameters								
	Carbon and oxygen atoms Binding energy (eV)	C1 283.6	C2 284.8	C3 286.0	C4 287.0	C5 288.7	O1 531.7	O2 533.2	O3 534.6
PET R	Atomic concentration (%)	2.3	51.1	16.8	13.8	16.0	46.7	46.5	6.8
PET RM	Atomic concentration (%)	1.7	56.2	23.4	9.3	9.4	64.0	36.0	–
PET RCM	Atomic concentration (%)	4.9	60.3	18.2	6.2	10.4	64.3	35.7	–

Table 4 Theoretical values of carbon, oxygen, and nitrogen atomic concentrations (%) and atomic ratios for chitosan, PNIAA and **CM** complexes, and polyester surface coverage based on N/C ratios

Values calculated assuming stoichiometric analogies among components and repeating units of *N*-isopropylacrylamide and acrylic acid	Atomic concentrations (%)			Atomic ratios		Polyester surface coverage (%)	
	C 1*s*	O 1*s*	N 1*s*	O/C	N/C	PET RM	PET RCM
Chitosan (acetylation degree: 5%)	54.7	36.3	9.0	0.66	0.16	–	38
PNIAA	69.2	23.1	7.7	0.33	0.11	82	55
CM complex	62.5	29.2	8.3	0.47	0.13	–	46

are found in stoichiometric analogy of 1:1 in PNIAA. Similarly, the theoretical values for a **CM** complex were calculated based on a 1:1 analogy of chitosan to PNIAA. Similar assumptions are reported in literature for copolymers of unknown degree of polymerization, based on which the grafting extent on surfaces or the surface fraction covered by a copolymer is determined [28]. If the PET RM surface was completely covered by PNIAA microparticles, its N/C ratio should be equal to the theoretical value of the PNIAA N/C ratio. Similarly, if the PET RCM surface was completely covered by **CM** complexes, its N/C ratio should be equal to the theoretical value of the **CM** complex N/C ratio. Therefore, by dividing the experimental N/C ratios found for PET RM and PET RCM (Table 2) by the corresponding theoretical N/C ratios of PNIAA and **CM** complexes (Table 4), respectively, the polyester surface coverage by microgels can be roughly estimated. A similar approach was reported in literature for poly(acrylic acid) grafted on polyamide 6,6 [29]. In the case of PET RM, the surface coverage was found to be 82%, whereas in the case of PET RCM, 46%. For the latter polyester, the surface coverage was also calculated considering the extreme possibilities that only chitosan is present on PET or only PNIAA microparticles, instead of **CM** complexes. In all three possibilities, it is shown that approximately only half of the PET RCM surface was covered after functionalization.

From the graph of the textile ζ-potential changes with pH in Fig. 2, it is clearly seen that PET RM has lower negative values than PET R between pH 4 and 10. Hence, functionalization with microgel **M** reduces the surface charge of polyester. Moreover, above pH 5, the ζ-potential practically stabilizes in the case of PET RM, a result in accordance with the electrophoretic mobility data of microgel **M** [11]. In the case of PET RCM, the ζ-potential has positive values up to almost pH 5.5, a result which confirms the presence of chitosan on the polyester surface. The zero surface-charge point for PET RCM appears at pH 5.5. This value is within the physiological pH range of human skin [30]. If the polyester surface was completely covered by **CM** complexes, then the zero-charge point of PET RCM would be expected to appear at pH 6, as the

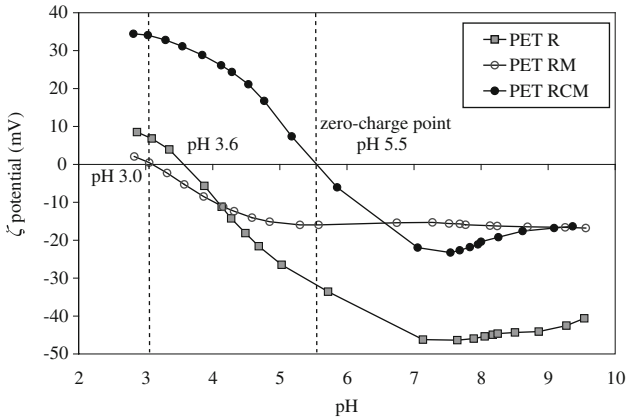

Fig. 2 ζ-potential changes with pH for the polyester textile samples PET R, PET RM, and PET RCM, determined through streaming potential measurements performed with an electrokinetic analyzer

isoelectric point of microgel **CM** is at pH 6 [11]. The appearance of the zero-charge point at lower pH suggests partial coverage [31–33]; this suggestion is corroborated by the corresponding SEM images of Fig. 1 and the XPS results of Table 4. Above pH 5.5, the ζ-potential of PET RCM decreases gradually to negative values and stabilizes around pH 9. In fact, the final value that it reaches coincides with the final value of PET RM. This observation indicates that, apart from chitosan, also PNIAA microparticles are present on the PET RCM surface, as the absolute values of ζ potential depend on charge density, as well as on the type of charged species [31, 33, 34]. If only chitosan was present on polyester without PNIAA, it would be deprotonated at pH 9 and it would not contribute to ζ potential. Thus, the ζ potential of PET RCM above pH 9 would be expected, in that case, to reach values close to the ones of PET R, not coincide with the ones of PET RM.

After SEM analysis for the surface morphology, XPS for the surface chemical composition and electrokinetic analysis for the surface charge, surface analysis of the polyester samples was completed with topographic measurements. Data derived from these measurements regarded dimensional changes of the textiles (relaxation, shrinkage) after functionalization, macro- and microroughness, as well as macro- and microporosity. The results are given in Table 5.

Macroroughness is expressed as the overall waviness of the textiles and microroughness as the average arithmetic roughness (R_a) of the filament surface in the warp and weft direction of the textiles. Macroporosity refers to the inter-yarn average pore size (throughout the whole textile surface) and microporosity to the intra-yarn average pore size (within the yarns in the warp and weft direction of the textiles). Note that in the case of macroroughness and macroporosity, no standard deviation is provided, as calculations were performed based on a single topographic substrate. However, the values obtained are considered valid for comparison because every sample was analyzed on the basis of 1,440,000 points (1200 × 1200 points evaluated). Therefore, the sample area used for the determination of macroroughness (waviness) and macroporosity is considered sufficiently large to yield results with minimized error.

As shown in Table 5, the woven structure of functionalized polyester textiles PET RM and PET RCM undergoes relaxation compared with the reference PET R. This means that the overall distance among yarns increases, even though no mechanical force was used during the microgel incorporation. In addition, the textile waviness decreases by approximately 11% for PET RM and by 30% for PET RCM. This means practically that the polyester surface becomes more even after the microgel incorporation. The macroporosity at the same time increases considerably for PET RM but remains almost unchanged for PET RCM. When comparing the macrotopography of the samples, it is necessary to consider these three parameters together and not individually. In the case of PET RM, the dimensional increase along the x axis (reflected in the relaxation observed) is followed or caused by a decrease in the y axis (reflected in waviness), which is normal if no compaction of the material occurs. The fact that also the inter-yarn pores appear bigger for PET RM than for PET R suggests that the expansion of the polyester textile structure was indeed caused by the microgel **M** incorporation. The reason is possibly that the dense PNIAA microparticle layer formed on the polyester fibers (as shown by SEM, Fig. 1b), pushed the yarns apart from one another during functionalization (i.e., when PNIAA microparticles were wet and swollen). Upon drying, the layer collapsed leaving bigger voids among the yarns than the initial ones. Considering that this polyester textile is thermo-fixed and thermo-stable (according to production company specifications), no shrinkage affects the dimensional changes observed. In the case of PET RCM, the fabric structure is more expanded and its surface more even than for PET RM, but the macroporosity is unaffected compared with PET R. This is supported by the SEM image for PET RCM (Fig. 1c) which shows **CM** complexes completely flattened on the fiber surface and in a less dense distribution than in the case of PET RM, neither blocking the inter-yarn pores nor expanding them. However, the microporosity for both PET RM and PET RCM is increased compared with PET R, in both the warp and weft direction. This suggests that the intra-yarn structure loosens and expands, as well. The increased microroughness along the warp filaments of PET RM is attributed to the presence of multiple PNIAA microparticles closely packed next to each other, as shown by SEM in Fig. 1b. The fact that there is no microroughness increase in the warp filaments of PET RCM is supported also by the SEM analysis which shows the **CM** complexes having no volume and being completely incorporated into the surface layer. However, the increased microroughness of the weft filaments compared with the warp ones, for both samples PET RM and PET RCM, could be attributed to the fact that the weft filaments are textured (not flat) by production; therefore, their innate roughness might have affected the results.

Testing the polyester pH/thermo-responsiveness in terms of water/moisture management

Having proven the incorporation of pH/thermo-responsive microgels into the polyester surface layer and investigated the effect of functionalization on the polyester surface properties, the performance of the functionalized polyester textiles was tested in terms of water absorption, water vapor transmission, and moisture regain at various conditions of temperature and RH. The results are shown in Table 6, Figs. 3 and 4, respectively.

In Table 6, it is shown that, among the three polyesters under study, PET RM has the highest total absorption times

Table 5 Topographical data of polyester textiles obtained through optical white-light scanning with a chromatic sensor

Sample	Textile topography			Yarn topography		Filament topography	
	Dimensional change (%)	Macroroughness (waviness) (μm)	Macroporosity ($\mu m^3/\mu m^2$)	Microporosity		Microroughness, R_a	
				Warp ($\mu m^3/\mu m^2$)	Weft ($\mu m^3/\mu m^2$)	Warp (nm)	Weft (nm)
PET R	0.0 (reference)	115	0.709	0.515 ± 0.129	0.344 ± 0.078	23 ± 6	41 ± 22
PET RM	6.5 ± 0.2 (relaxation)	102	0.927	0.584 ± 0.195	0.431 ± 0.064	30 ± 11	44 ± 16
PET RCM	9.7 ± 0.8 (relaxation)	82	0.702	0.726 ± 0.143	0.438 ± 0.115	19 ± 5	57 ± 6

Table 6 Total absorption times of the polyester textile samples PET R, PET RM, and PET RCM, determined at different pH with a dynamic contact angle tester

Polyester textile samples	Total absorption time (s)		
	Buffer solution (pH 4)	Water (pH 6.4)	Buffer solution (pH 8)
PET R	43 ± 12	32 ± 9	45 ± 25
PET RM	157 ± 10	137 ± 31	97 ± 47
PET RCM	10 ± 1	12 ± 2	5 ± 2

at all studied pH, and PET RCM the lowest. This difference can be attributed not only to the different chemical composition of the microgels, but also to their distribution on the fibers. Microgel **M** which forms a continuous layer on the fibers is the first material to come in contact with the drop in the case of PET RM; apparently, **M** (i.e., PNIAA) microparticles need more time to absorb water, which will cause them to become gradually ionized and swollen. Hence, PET RM takes longer time to absorb the drop than if the water was in direct contact with the textile structure and could diffuse into the pores, as in the case of reference PET R. The increase in water absorption times due to the microparticle presence is also supported by the increased microroughness observed for PET RM, as described previously through the topographical data. In the case of PET RCM, where the **CM** complexes do not cover the fibers completely, water can be absorbed both by the **CM** microgel and the textile structure, leading to shorter total absorption times.

Regarding the pH responsiveness of the functionalized textiles, the presence of microgels **M** and **CM** seems to have a significant effect on the textile absorption times. When pH increases from 4 to 8, the total absorption time for PET RM decreases as a consequence of the PNIAA gradual ionization above pH 4 [11]. However, it should be noted that the statistical error of measurement also increased with pH, eventually leading to time values of the same order of magnitude. This result can be attributed to the fact that while PNIAA microparticles become extensively ionized between pH 6 and 8, consequently, the surface of polyester PET RM becomes increasingly negatively charged. As shown in Fig. 2, this polyester surface ionization reaches plateau in the alkaline region, but its onset appears around pH 6. Therefore, similarities among the PET RM total absorption times, particularly between pH 6 and 8, are not surprising. The standard errors could also reflect local irregularities of the microparticle distribution on the fibers and of their subsequent compaction as they swell with increasing pH. The fact that reference polyester PET R does not behave similarly, even though its surface is also increasingly negatively charged, could be attributed to the different nature of its carboxyl end groups compared with that of PET RM. Although acrylic acid (component of PNIAA and therefore **M**) is a weak acid, in its polymeric form it uses its multiple carboxyl groups to attract large amounts of water [35], especially when fully ionized. Therefore, the difference in absorption times is more evident for PET RM than for PET R. For PET RCM, the lowest total absorption time is also observed at pH 8, like for PET RM. However, at pH 4 its total absorption time is lower than at neutral pH, unlike for PET RM. This can be attributed to the simultaneous ionization of both chitosan and PNIAA on the surface of PET RCM, even though this ionization occurs at different degrees for each component. At pH 4, chitosan amine groups are highly protonated, whereas PNIAA carboxylic groups are just starting to be ionized. At pH 8, on the other hand, chitosan amine groups are almost completely deprotonated, whereas PNIAA carboxylic groups are fully ionized. This synergistic interaction possibly leads to lower total absorption times for PET RCM in both the acidic and alkaline region, compared with the corresponding times for PET R and PET RM. A contributing factor to this effect is also the topography of PET RCM, described previously with characteristics such as expanded structure (relaxation), decreased macroroughness and increased microporosity, compared with PET R and PET RM.

Regarding water vapor transmission, at 65% RH the functionalized polyesters PET RM and PET RCM have higher transmission rates than reference polyester PET R, both at 20 and 40 °C (Fig. 3a). In the case of PET RM, this result is attributed to two factors; the increased textile macroporosity after functionalization (Table 5), and the microgel presence on the polyester fibers which helps attract more moisture. For PET RCM, the second factor seems to play the main role, as the macroporosity remained practically unaffected after functionalization. This latter result of increased WVTR at 65% RH owing to the CM presence on PET RCM is supported by findings of another study which uses microgel CM for functionalization of aminated polyester [36].

When RH rises to 95% (Fig. 3b), all polyester samples have much lower WVTR than their corresponding rates at 65% RH. This result is expected because the higher the humidity is, the smaller becomes the driving force for vapor transmission. This driving force is, in fact, the difference between the amounts of moisture in the spaces below and above the textile sample [37]. At 40 °C and 95% RH, the functionalized polyesters—PET RM in particular—have lower WVTR than reference PET R, owing to the thermo-responsive nature of PNIAA microparticles which become hydrophobic above 36 °C. At 20 °C and 95% RH,

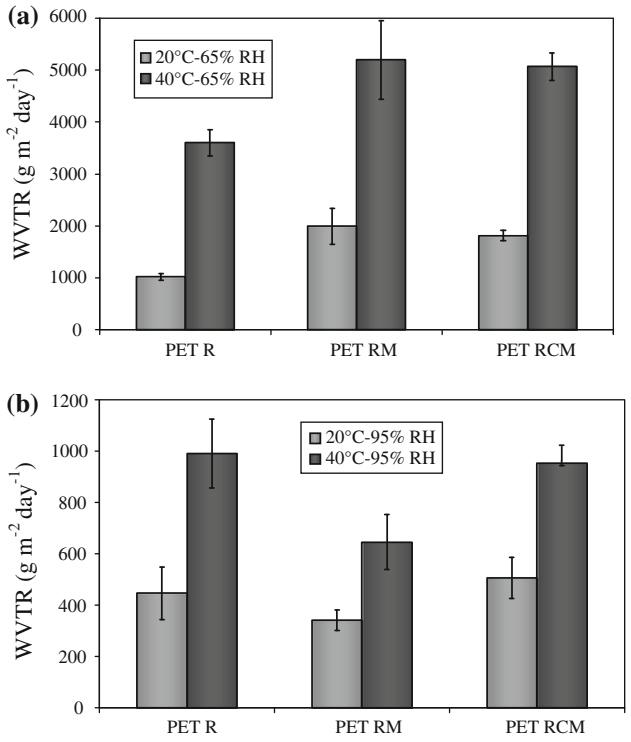

Fig. 3 Water vapor transmission rates for polyester textile samples PET R, PET RM, and PET RCM, below and above the PNIAA LCST and at 65% RH (**a**) and 95% RH (**b**)

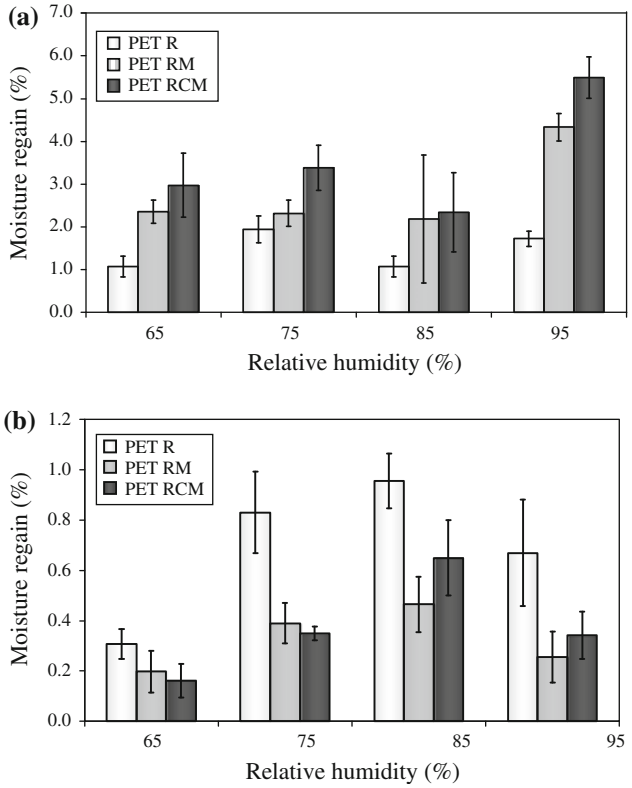

Fig. 4 Moisture regains of polyester textile samples PET R, PET RM, and PET RCM, at various RH values and at 20 °C (**a**) and 40 °C (**b**)

PET RCM has higher WVTR than PET R, as expected, because of the microgel presence on the fibers. However, at the same conditions PET RM has the lowest WVTR among the three samples, even though its macroporosity—which affects permeability [38]—was found to be bigger than that of PET R and PET RCM. This peculiarity can be attributed to the fact that microgel **M** forms a continuous layer on the fibers; as the PNIAA microparticles become increasingly swollen due to high RH, they possibly block the polyester pores hindering vapor transmission.

The thermo-responsiveness of the functionalized polyesters can be evaluated better through the moisture regain results presented in Fig. 4. At 20 °C, PET RCM has the highest moisture regain compared with both PET R and PET RM. Moreover, for the functionalized polyesters PET RM and PET RCM, moisture regain has the highest value at 95% RH and, strangely enough, a minimum at 85% RH. This result suggests that there is a critical point of RH at which two phenomena compete; drying rate due to evaporation, and moisture uptake due to microgel swelling and to absorption from the textile itself. Below that point, i.e., at 65 and 75% RH, moisture absorption prevails even though hindered by simultaneous drying. Above that point, evaporation is limited due to high levels of ambient moisture and therefore absorption is predominant, leading up to almost 6% of moisture regain for PET RCM.

As expected, at 40 °C and due to the PNIAA thermo-responsive nature, the functionalized polyesters PET RM and PET RCM have lower moisture regains than reference polyester PET R. The contribution of the hydrophobic character of PNIAA above its LCST to decreased moisture regains of polyester is more noticeable at high RH, i.e., 95%, where drying is not as intense as at lower RH. These results combined with the lower WVTR of PET RM and PET RCM at 40 °C show clearly that polyester textiles functionalized with PNIAA microparticles (whether alone in suspension or complexed with chitosan) exhibit thermo-responsiveness at a temperature range close to the average human body temperature.

Conclusions

A new path for functionalizing polyester textiles was proposed in this study. It involved incorporation of pH/thermo-responsive microgels into the polyester surface layer through UV irradiation. It was confirmed by SEM and XPS that PNIAA microparticles and **CM** complexes were incorporated into the fiber surface layer. It was also estimated through XPS data and theoretical values that the

polyester surface coverage by microgels **M** and **CM** was almost double for PET RM (82%) compared with PET RCM (46%), respectively. Furthermore, electrokinetic analysis and dynamic wetting measurements at different pH values revealed that pH-responsiveness was imparted from the microgels to the polyester textiles. More specifically, the change in the PET RCM surface charge from positive to negative values occurred at pH 5.5, close to the **CM** microgel isoelectric point. This pH value approximates the average pH of human skin, confirming that the functionalized polyester is pH-responsive within a physiological pH range. Furthermore, total absorption times for PET RM decreased with increasing pH, but were still much longer than those for PET R and PET RCM. The latter polyester had the shortest total absorption times at all studied pH. To this result contributed also its topographical characteristics such as its expanded structure, decreased macroroughness, and increased microporosity, compared with the corresponding parameters of the other two samples. The thermoresponsiveness of the functionalized polyesters PET RM and PET RCM was confirmed through their decreased moisture regains at 40 °C (i.e., above the microgel LCST and volume/phase transition from expanded/hydrophilic to shrunken/hydrophobic state), compared with reference polyester PET R. Moreover, at 40 °C and low RH, the water vapor transmission rates were higher for the functionalized polyesters than for the reference, and lower at 40 °C and high RH. This supports the conclusion of imparted thermoresponsiveness because at low RH drying through evaporation is more pronounced than at high RH. Therefore, the contribution of the microgel hydrophobic character to the water vapor transmission rate of polyester at 40 °C was more clearly distinguished at high RH.

Acknowledgements Financial support for this work was provided by the project ADVANBIOTEX (MEXT-CT-2006-042641), a Marie Curie Excellence Grant (EXT) funded by the EU's FP6 Programme. The authors would also like to thank Mrs. Anja Caspari from the Leibniz-Institut für Polymerforschung Dresden e.V. in Germany for the textile electrokinetic measurements.

References

1. Solga A, Cerman Z, Striffler B, Spaeth M, Barthlott W (2007) Bioinsp Biomim 2:126
2. Sim KJ, Han SO (2010) Macromol Res 18:489
3. Egusa S, Wang Z, Chocat N, Ruff ZM, Stolyarov AM, Shemuly D, Sorin F, Rakich PT, Joannopoulos JD, Fink Y (2010) Nat Mater 9:643
4. Harlin A, Nousiainen P, Puolakka A, Pelto J, Sarlin J (2005) J Mater Sci 40:5365. doi:10.1007/s10853-005-4333-1
5. Buyle G (2009) Mater Technol 24:46
6. Xue CH, Jia ST, Zhang J, Tian LQ (2009) Thin Solid Films 517:4593
7. Jones CD, Lyon LA (2000) Macromolecules 33:8301
8. Fujii A, Maruyama T, Sotani T, Ohmukai Y, Matsuyama H (2009) Colloids Surf A 337:159
9. Pelton R (2000) Adv Colloid Interface Sci 85:1
10. Jayakumar R, Menon D, Manzoor K, Nair SV, Tamura H (2010) Carbohydr Polym 82:227
11. Glampedaki P, Krägel J, Petzold G, Dutschk V, Miller R, Warmoeskerken MMCG Polyester textile functionalization through incorporation of pH/thermo-responsive microgels. Part I: Microgel preparation and characterization (submitted)
12. Ranby B (1998) Polym Eng Sci 38:1229
13. Lopergolo LC, Lugao AB, Catalani LH (2003) Polymer 44:6217
14. He D, Susanto H, Ulbricht M (2009) Prog Polym Sci 34:62
15. Tran-Cong Q, Nagaki T, Yano O, Soen T (1991) Macromolecules 24:1505
16. Fechine GJM, Rabello MS, Souto Maior RM, Catalani LH (2004) Polymer 45:2303
17. Yang W, Ranby B (1996) J Appl Polym Sci 62:545
18. Hawkins CL, Davies MJ (2001) Biochim Biophys Acta 1504:196
19. Turecek F, Syrstad EA (2003) J Am Chem Soc 125:3353
20. Andrady AL, Torikai A, Kobatake T (1996) J Appl Polym Sci 62:1465
21. Stawski D, Bellmann C (2009) Colloids Surf A 345:191
22. Calvimontes A, Dutschk V, Stamm M (2010) Text Res J 80:1004
23. Hasan MMB, Calvimontes A, Synytska A, Dutschk V (2008) Text Res J 78:996
24. Zhua Z, Kelley MJ (2004) Appl Surf Sci 236:416
25. Lang FR, Pitton Y, Mathieu HJ, Landolt D, Moser EM (1997) Fresenius J Anal Chem 358:251
26. Yang CQ, Bresee RR, Fateley WG (1990) Appl Spectrosc 44:1035
27. Curti PS, de Moura MR, Veiga W, Radovanovic E, Rubira AF, Muniz EC (2005) Appl Surf Sci 245:223
28. Zekonyte J, Williams RL, Beamson G, Weightman P (2009) Surf Interface Anal 41:316
29. Tobiesen FA, Michielsen S (2002) J Polym Sci A 40:719
30. Schneider LA, Korber A, Grabbe S, Dissemond J (2007) Arch Dermatol Res 298:413
31. Goddard JM, Hotchkiss JH (2007) Prog Polym Sci 32:698
32. Luxbacher T (2010) Prüfen und Messen (Test Measuring) 2010:74
33. Stakne K, Smole MS, Kleinschek KS, Jaroschuk A, Ribitsch V (2003) J Mater Sci 38:2167. doi:10.1023/A:1023776030473
34. Lettmann C, Moeckel D, Staude E (1999) J Membr Sci 159:243
35. Brannon-Peppas L, Harland RS (1990) Superabsorbent polymer technology. Elsevier, Amsterdam
36. Glampedaki P, Dutschk V, Jocic D, Warmoeskerken MMCG (2011) Biotechnol J 6(10):1219
37. Huang J, Chen Y (2010) Text Res J 80:422
38. Ogulata RT, Mavruz S (2010) Fibres Text East Europe 18:71